Eur. Phys. J. A (2013) **49**: 33
DOI 10.1140/epja/i2013-13033-8

THE EUROPEAN PHYSICAL JOURNAL A

Regular Article – Theoretical Physics

Investigations of spinodal dynamics in asymmetric nuclear matter within a stochastic relativistic model

O. Yilmaz[1,a], S. Ayik[2,b], F. Acar[1], S. Saatci[1], and A. Gokalp[3]

[1] Physics Department, Middle East Technical University, 06800 Ankara, Turkey
[2] Physics Department, Tennessee Technological University, Cookeville, TN 38505, USA
[3] Department of Physics, Bilkent University, 06800 Ankara, Turkey

Received: 25 October 2012 / Revised: 18 December 2012
Published online: 12 March 2013 –
Communicated by A. Schwenk

Abstract. Early development of spinodal instabilities and density correlation functions in asymmetric nuclear matter are investigated in the stochastic extension of the Walecka-type relativistic mean field including coupling with rho meson. Calculations are performed under typical conditions encountered in heavy-ion collisions and in the crusts of neutron stars. In general, growth of instabilities occur relatively slower for increasing charge asymmetry of matter. At higher densities around $\rho = 0.4\rho_0$ fluctuations grow relatively faster in the quantal description than those found in the semi-classical limit. Typical sizes of early condensation regions extracted from density correlation functions are consistent with those found from dispersion relations of the unstable collective modes.

1 Introduction

The stochastic mean-field (SMF) approach in either non-relativistic or relativistic frameworks is different from the standard mean-field theory due to the different initial conditions employed. The standard mean-field theory with a well-defined initial condition provides a deterministic description for the nuclear collision dynamics. On the other hand, in the SMF approach quantal and thermal fluctuations at the initial state are incorporated in a stochastic manner by generating an ensemble of single-particle densities according to the self-consistent mean-field evolution of each event. Therefore the SMF approach provides a probabilistic description of the nuclear collision dynamics [1]. Once an ensemble of the single-particle density matrices are generated, we can calculate the expectation values and the variances of the observables by taking the averages over the ensemble. It is demonstrated that the SMF approach describes nuclear collision dynamics at low energies including one-body dissipation and fluctuation mechanisms in accordance with the quantal dissipation-fluctuation relation [1]. It is shown that for small amplitude fluctuations the SMF approach gives rise to the same result as the one deduced from a variational approach for dispersion of one-body observables [2]. Also, transport coefficients for macroscopic variables deduced from the SMF approach have the same form with those familiar from the phenomenological nucleon-exchange model for deep-inelastic collisions [3–5]. As a further testing, in a recent work the approach is applied to the Lipkin-Meshkov model, which has an exact quantal solution [6]. It is illustrated that the SMF approach well describes the gross properties of exact quantal evolution. All these demonstrations support that the SMF approach provides a useful tool for describing deep inelastic heavy-ion collisions, heavy-ion fusion near barrier energies, spinodal decomposition of nuclear systems in which mean-field fluctuation mechanisms play a dominant role.

We recently investigated early development spinodal dynamics [7] and baryon density correlation functions in symmetric nuclear matter in the semi-classical [8,9], and also in quantal frameworks [10]. We carried out these studies by employing stochastic extension of the Walecka-type relativistic mean-field model including the self-interaction of scalar mesons [10–14]. In these studies, we examined the early development of spinodal instabilities and baryon density correlation functions in the ideal case of charge-symmetric nuclear matter for relevant values of initial densities and temperatures. In the present study, we extend our investigations to examine the early development of spinodal dynamics in charge-asymmetric nuclear matter employing the stochastic extension of the relativistic mean-field theory by including coupling of baryon fields to rho mesons. As in previous studies, we carry out these calculations in both quantal and semi-classical frameworks of the relativistic mean-field approach. We note that the formal presentation of this work and notation are similar to

[a] e-mail: oyilmaz@metu.edu.tr
[b] e-mail: ayik@tntech.edu

the treatment presented in previous works [8–10]. Therefore we provide a short description of the formalism here and for details, please refer to refs. [8–10]. In sect. 2, we briefly describe the stochastic extension of the relativistic mean-field approach including rho meson coupling in the quantal framework and develop a linear response treatment for spinodal instabilities. In sect. 3, we present the results of calculations for early development of baryon density correlation functions in different charge-asymmetric nuclear matter. In sect. 4, conclusions are given.

2 Relativistic mean field including rho mesons

For our purpose, it is most convenient to formulate the relativistic mean-field theory in terms of single-particle density matrix. Starting from a well-defined initial distribution, we need to generate an ensemble of single-particle density matrices, $\{\rho_\alpha^{(n)}(t)\}$, where n indicates the event label. Time evolution of each member of the relativistic single-particle density matrix is determined by its own self-consistent mean field $h_\alpha(\rho^{(n)})$ [13],

$$i\hbar\frac{\partial}{\partial t}\rho_\alpha^{(n)}(t) = \left[h_\alpha(\rho^{(n)}),\ \rho_\alpha^{(n)}(t)\right]. \tag{1}$$

This equation is formally similar to the non-relativistic TDHF equation for the single-particle density matrix. However, we should note that here $\rho_\alpha(t)$ is a 4×4 matrix in the spinor space and $h_\alpha(\rho^{(n)})$ denotes the relativistic mean-field Hamiltonian in the event n. For simplicity, in the rest of the paper, we ignore the event label n on the density matrix, and label $\alpha = p, n$ denotes protons and neutrons. In this work, we employ the Walecka model including non-linear self-coupling terms of scalar meson and coupling to charged rho mesons [15]. As a result, relativistic mean-field Hamiltonians for protons and neutrons are given by

$$h_p(\rho) = \vec{\alpha}\cdot\left[c\vec{p} - g_{\rm v}\vec{V} - \frac{1}{2}g_\rho\vec{b}_3 - e\vec{A}\right] + \beta(Mc^2 - g_{\rm s}\phi) + g_{\rm v}V_0 + \frac{1}{2}g_\rho b_{3,0} + eA_0, \tag{2}$$

and

$$h_n(\rho) = \vec{\alpha}\cdot\left[c\vec{p} - g_{\rm v}\vec{V} + \frac{1}{2}g_\rho\vec{b}_3\right] + \beta(Mc^2 - g_{\rm s}\phi) + g_{\rm v}V_0 - \frac{1}{2}g_\rho b_{3,0}. \tag{3}$$

Here $\vec{\alpha}$ and β are Dirac matrices, ϕ, $V_\mu \equiv (V_0, \vec{V})$, $A_\mu \equiv (A_0, \vec{A})$ and $B_{3\mu} \equiv (b_{3,0}, \vec{b}_3)$ scalar meson, neutral vector meson, electro-magnetic and z-component of charged rho meson fields, and $g_{\rm s}$, $g_{\rm v}$ and g_ρ are the corresponding coupling constants, respectively. We note that the coupling constants in these expressions are obtained from the standard coupling constants as follows: $g_{\rm s} \to g_{\rm s}\sqrt{\hbar c}$, $g_{\rm v} \to g_{\rm v}\sqrt{\hbar c}$, $g_\rho \to g_\rho\sqrt{\hbar c}$, and also $g_2 \to g_2/\sqrt{\hbar c}$, $g_3 \to g_3/\hbar c$, for coupling constants of non-linear terms in the scalar meson field. Since the nuclear system has well-defined electric charge only the third component of the rho meson field appears in the equation of motion. The meson field obeys the usual Klein-Gordon equations with source terms determined by fluctuating scalar $\rho_\alpha^{\rm s}(\vec{r},t)$, baryon $\rho_\alpha^{\rm b}(\vec{r},t)$ and current $\vec{\rho}_\alpha^{\rm v}(\vec{r},t)$ densities [12]. These fluctuating densities are defined by

$$\begin{pmatrix}\vec{\rho}_\alpha^{\rm v}(\vec{r},t)\\ \rho_\alpha^{\rm b}(\vec{r},t)\\ \rho_\alpha^{\rm s}(\vec{r},t)\end{pmatrix} = \sum_{ij}\Psi_{\alpha,j}^\dagger(\vec{r},t)\begin{pmatrix}c\vec{\alpha}\\ 1\\ \beta\end{pmatrix}\Psi_{\alpha,i}(\vec{r},t)\rho_{ij}(\alpha), \tag{4}$$

where summations i, j run over a complete set of spinors $\Psi_{\alpha,i}(\vec{r},t)$ and $\rho_{ij}(\alpha)$ indicates the time-independent elements of the single-particle density matrix. According to the SMF approach, the elements of the density matrix are uncorrelated Gaussian random numbers with mean values $\overline{\rho}_{ij}(\alpha) = \delta_{ij}n_j(\alpha)$, and variances are given by

$$\overline{\delta\rho_{ij}(\alpha)\delta\rho_{j'i'}(\alpha')} = \frac{1}{2}\delta_{\alpha\alpha'}\delta_{ii'}\delta_{jj'}\big\{n_i(\alpha)[1-n_j(\alpha)] + n_j(\alpha)[1-n_i(\alpha)]\big\}, \tag{5}$$

where $n_j(\alpha)$ are the occupation numbers of single-particle spinors.

For investigation of the early growth of density fluctuations in the spinodal region, it is sufficient to consider the linear response treatment of dynamical evolution. The small-amplitude fluctuations of the single-particle density matrix around an equilibrium initial state with proton and neutron density matrices, $(\rho_p^0, \rho_n^0) \equiv \rho_0$, are determined by the linear limit of the relativistic mean-field eq. (1). The linearized mean-field equation for the fluctuating density matrices for protons and neutrons $\delta\rho_\alpha(t) = \rho_\alpha(t) - \rho_\alpha^0$ becomes

$$i\hbar\frac{\partial}{\partial t}\delta\rho_\alpha(t) = [h_\alpha(\rho_0),\ \delta\rho(t)] + [\delta h(t),\ \rho_\alpha^0], \tag{6}$$

where

$$h_p(\rho_0) = \vec{\alpha}\cdot c\vec{p} + \beta(Mc^2 - g_{\rm s}\phi_0) + g_{\rm v}V_0 + \frac{1}{2}g_\rho b_{3,0} \tag{7}$$

and

$$h_n(\rho_0) = \vec{\alpha}\cdot c\vec{p} + \beta(Mc^2 - g_{\rm s}\phi_0) + g_{\rm v}V_0 - \frac{1}{2}g_\rho b_{3,0} \tag{8}$$

represent the mean-field Hamiltonian for protons and neutrons in the initial state, respectively. Since, in the initial state, average baryon and scalar densities are assumed to be uniform, there are the following relations between initial densities and the meson fields:

$$\mu_{\rm s}^2\phi_0 = g_{\rm s}(\rho_{p,0}^{\rm s} + \rho_{n,0}^{\rm s}) + 2g_2\phi_0 + 3g_3\phi_0^2, \tag{9}$$

$$\mu_{\rm v}^2 V_0 = g_{\rm v}(\rho_{p,0}^{\rm b} + \rho_{n,0}^{\rm b}) \tag{10}$$

and

$$\mu_\rho^2 b_{3,0}^0 = g_\rho(\rho_{p,0}^{\rm b} - \rho_{n,0}^{\rm b}). \tag{11}$$

In these expressions $\rho^{\rm s}_{p,0}$, $\rho^{\rm s}_{n,0}$, $\rho^{\rm b}_{p,0}$ and $\rho^{\rm b}_{n,0}$ are scalar and baryon densities for protons and neutrons in the initial state, respectively, and $\vec{V}^0 = 0$, $\vec{b}^0_3 = 0$, $A^0_0 = 0$. The fluctuating parts of the mean-field Hamiltonian for protons and neutrons in eq. (6) are given by

$$\begin{aligned}\delta h_p(t) = &-\vec{\alpha}\cdot\left[g_{\rm v}\delta\vec{V}(\vec{r},t) + \frac{1}{2}g_\rho\delta\vec{b}_3(\vec{r},t) + e\delta\vec{A}(\vec{r},t)\right]\\ &-\beta g_{\rm s}\delta\phi(\vec{r},t) + g_{\rm v}\delta V_0(\vec{r},t)\\ &+\frac{1}{2}g_\rho\delta b_{3,0}(\vec{r},t) + e\delta A_0(\vec{r},t) \qquad (12)\end{aligned}$$

and

$$\begin{aligned}\delta h_n(t) = &-\vec{\alpha}\cdot\left[g_{\rm v}\delta\vec{V}(\vec{r},t) - \frac{1}{2}g_\rho\delta\vec{b}_3(\vec{r},t)\right] - \beta g_{\rm s}\delta\phi(\vec{r},t)\\ &+g_{\rm v}\delta V_0(\vec{r},t) - \frac{1}{2}g_\rho\delta b_{3,0}(\vec{r},t). \qquad (13)\end{aligned}$$

The small-amplitude fluctuation of meson fields evolves according to the linearized Klein-Gordon equation, for details please see [10].

The analysis of the linear response treatment of the instabilities in nuclear matter is relatively simple and it can be carried out in a nearly analytical framework. In this case, the plane wave representation of spinors for protons and neutrons, $\alpha = p, n$, provides a suitable representation for the quantal investigation of the instabilities. Positive-energy ($\lambda = +1$) and negative-energy ($\lambda = -1$) plane wave spinors with spin quantum number $s = \pm 1/2$ can be expressed as

$$|\psi_{\alpha,\lambda}(\vec{p},s)\rangle = N_{\alpha,\lambda}(\vec{p})\begin{pmatrix}\chi_{\alpha,s}\\ \frac{\vec{\sigma}\cdot c\vec{p}}{Mc^2+\lambda e^*(p)}\chi_{\alpha,s}\end{pmatrix}|e^{i\vec{p}\cdot\vec{r}/\hbar}\rangle. \quad (14)$$

Here, $\chi_{\alpha,s} = \binom{1}{0}$, $\binom{0}{1}$ denote spin states for protons and neutrons, the normalization factor is given by

$$N_{\alpha,\lambda}(\vec{p}) = \sqrt{[Mc^2 + \lambda e^*(\vec{p})]/2\lambda e^*(p)}. \qquad (15)$$

The quantity $e^*(p) = \sqrt{\vec{p}^2c^2 + M^{*2}c^4}$ denotes the effective single-particle energies in the initial state which is determined by the effective nucleon mass $M^*c^2 = Mc^2 - g_{\rm s}\phi_0$. These plane wave spinors are eigenstates of the mean-field Hamiltonian in the uniform initial state,

$$h_\alpha(\rho_0)|\psi_{\alpha,\lambda}(\vec{p},s)\rangle = E_{\alpha,\lambda}(\vec{p})|\psi_{\alpha,\lambda}(\vec{p},s)\rangle, \qquad (16)$$

with the eigenvalues $E_{p,\lambda}(p) = g_{\rm v}V_0 + \Delta E + \lambda e^*(\vec{p})$ for protons and $E_{n,\lambda}(p) = g_{\rm v}V_0 - \Delta E + \lambda e^*(\vec{p})$ for neutrons, where $\Delta E = (g_\rho/2m_\rho)^2(\rho^0_{p,b} - \rho^0_{n,b})$ denotes the single-particle energy shift due to the asymmetry energy. We expand the fluctuating density matrix in terms of plane wave spinor representation as follows:

$$\begin{aligned}\delta\rho_\alpha(t) = &\sum_{\lambda\lambda' s_2 s_1}\int\frac{{\rm d}^3p_1{\rm d}^3p_2}{(2\pi\hbar)^6}|\Psi_{\alpha,\lambda'}(\vec{p}_2,s_2)\rangle\delta\rho^{s_2s_1}_{\alpha,\lambda'\lambda}\\ &\times(\vec{p}_2,\vec{p}_1,t)\langle\Psi_{\alpha,\lambda}(\vec{p}_1,s_1)|. \qquad (17)\end{aligned}$$

We analyze the density fluctuations in the no-sea approximation. In the spinor space there are four different energy sectors $(\lambda,\lambda') = (+,+)$, $(-,+)$, $(+,-)$, $(-,-)$ corresponding to positive-energy particle hole excitations above the Fermi level, negative-energy particle positive-energy hole, negative-energy hole positive-energy particle and particle hole excitations within the Dirac sea, respectively. Thus in the no-sea approximation, occupation numbers of unoccupied states at zero temperature are zero and are very small at low temperatures. In ref. [13], it was shown that particle hole excitations corresponding to the $(-,+)$ and $(+,-)$ sectors make sizable contributions on the excitation strength of giant collective vibrations. According to our previous study, for symmetric matter, we found that, at low temperatures, contributions to unstable collective modes arising from the $(-,+)$ and $(+,-)$ sectors for early density fluctuations are less than 10%. Since magnitude of these contributions tends to increase for increasing charge asymmetry of the system, we include the $(-,+)$ and $(+,-)$ sectors in our calculations. We further simplify the description by considering the spin-averaged matrix elements of the fluctuating single-particle density matrix $\delta\rho_{\alpha,\lambda'\lambda}(\vec{p}_2,\vec{p}_1,t) = \frac{1}{2}\sum_s\delta\rho^{ss}_{\alpha,\lambda'\lambda}(\vec{p}_2,\vec{p}_1,t)$. Calculating the matrix element of eq. (6) between the spinors, we find for the fluctuating density matrix of protons and neutrons,

$$\begin{aligned}&i\hbar\frac{\partial}{\partial t}\delta\rho_{p,\lambda'\lambda}(\vec{p}_2,\vec{p}_1,t) =\\ &[\lambda' e^*(p_2) - \lambda e^*(p_1)]\,\delta\rho_{p,\lambda'\lambda}(\vec{p}_2,\vec{p}_1,t)\\ &+[n_{p\lambda}(p_1) - n_{p\lambda'}(p_2)]\Bigg\{-\vec{\xi}^v_{\lambda'\lambda}\cdot\Bigg[g_{\rm v}\delta\vec{V}(\vec{k},t)\\ &+\frac{1}{2}g_\rho\delta\vec{b}_3(\vec{k},t) + e\delta\vec{A}(\vec{k},t)\Bigg] - \xi^s_{\lambda'\lambda}g_{\rm s}\delta\phi(\vec{k},t)\\ &+\xi^b_{\lambda'\lambda}\left[g_{\rm v}\delta V_0(\vec{k},t) + \frac{1}{2}g_\rho\delta b_{3,0}(\vec{k},t) + e\delta A_0(\vec{k},t)\right]\Bigg\} \qquad (18)\end{aligned}$$

and

$$\begin{aligned}&i\hbar\frac{\partial}{\partial t}\delta\rho_{n,\lambda'\lambda}(\vec{p}_2,\vec{p}_1,t) =\\ &[\lambda' e^*(p_2) - \lambda e^*(p_1)]\delta\rho_{n,\lambda'\lambda}(\vec{p}_2,\vec{p}_1,t) + [n_{n\lambda}(p_1)\\ &-n_{n\lambda'}(p_2)]\Bigg\{-\vec{\xi}^v_{\lambda'\lambda}\cdot\left[g_{\rm v}\delta\vec{V}(\vec{k},t) - \frac{1}{2}g_\rho\delta\vec{b}_3(\vec{k},t)\right]\\ &-\xi^s_{\lambda'\lambda}g_{\rm s}\delta\phi(\vec{k},t) + \xi^b_{\lambda'\lambda}\left[g_{\rm v}\delta V_0(\vec{k},t) - \frac{1}{2}g_\rho\delta b_{3,0}(\vec{k},t)\right]\Bigg\}. \qquad (19)\end{aligned}$$

In these expressions, $n_{\alpha,\lambda}(p) = 1/[\exp(e^* - \lambda\mu^*_\alpha)/T + 1]$ denotes baryon occupation factors for positive- and negative-energy states with $\mu^*_\alpha = \mu_{\alpha,0} - (g_{\rm v}/\mu_{\rm v})^2\rho^b_{\alpha,0}$ where $\mu_{\alpha,0}$ and $\rho^b_{\alpha,0}$ are the chemical potential and baryon density of protons and neutrons $\alpha = p, n$ at the initial state, respectively, and $\mu_{\rm v}$ is the mass parameter of the vector meson. The quantities $\delta\vec{V}(\vec{k},t)$, $\delta V_0(\vec{k},t)$, $\delta\vec{A}(\vec{k},t)$, $\delta A_0(\vec{k},t)$, $\delta\phi(\vec{k},t)$, $\delta\vec{b}_3(\vec{k},t)$, and $\delta b_{3,0}(\vec{k},t)$ denote the space Fourier transforms of fluctuating vector and scalar meson fields, respectively, with $\hbar\vec{k} = \vec{p}_2 - \vec{p}_1$. The

$$\begin{pmatrix} A_1^p & A_2^p & A_3^p & A_1^n & A_2^n & A_3^n \\ B_1^p & B_2^p & B_3^p & B_1^n & B_2^n & B_3^n \\ C_1^p & C_2^p & C_3^p & C_1^n & C_2^n & C_3^n \\ D_1^p & D_2^p & D_3^p & D_1^n & D_2^n & D_3^n \\ E_1^p & E_2^p & E_3^p & E_1^n & E_2^n & E_3^n \\ F_1^p & F_2^p & F_3^p & F_1^n & F_2^n & F_3^n \end{pmatrix} = \begin{pmatrix} -P\chi_p^{\rm v} & -Q\chi_p^{\rm s} & 1+P\chi_p^{\rm b} & -G\chi_p^{\rm v} & -Q\chi_p^{\rm s} & G\chi_p^{\rm b} \\ -P\tilde{\chi}_p^{\rm v} & 1-Q\tilde{\chi}_p^{\rm s} & P\chi_p^{\rm s} & -G\tilde{\chi}_p^{\rm v} & -Q\tilde{\chi}_p^{\rm s} & G\chi_p^{\rm s} \\ 1-P\tilde{\chi}_p^{\rm b} & -Q\tilde{\chi}_p^{\rm v} & P\chi_p^{\rm v} & -G\tilde{\chi}_p^{\rm b} & -Q\tilde{\chi}_p^{\rm v} & G\chi_p^{\rm v} \\ -G\chi_n^{\rm v} & -Q\chi_n^{\rm s} & G\chi_n^{\rm b} & -R\chi_n^{\rm v} & -Q\chi_n^{\rm s} & 1+R\chi_n^{\rm b} \\ -G\tilde{\chi}_n^{\rm v} & -Q\tilde{\chi}_n^{\rm s} & G\chi_n^{\rm s} & -R\tilde{\chi}_n^{\rm v} & 1-Q\tilde{\chi}_n^{\rm s} & R\chi_n^{\rm s} \\ -G\tilde{\chi}_n^{\rm b} & -Q\tilde{\chi}_n^{\rm v} & G\chi_n^{\rm v} & 1-R\tilde{\chi}_n^{\rm b} & -Q\tilde{\chi}_n^{\rm v} & R\chi_n^{\rm v} \end{pmatrix}, \quad (27)$$

quantities $\vec{\xi}^{\rm v}_{\lambda'\lambda}(\vec{p}_2,\vec{p}_1)$, $\vec{\xi}^{\rm s}_{\lambda'\lambda}(\vec{p}_2,\vec{p}_1)$ and $\vec{\xi}^{\rm b}_{\lambda'\lambda}(\vec{p}_2,\vec{p}_1)$ are derived in the appendix A of [16] and given by eqs. (14)–(16) in this reference. We neglect a slight difference of these quantities for proton and neutron due to their effective masses. Also as seen from the same appendix A, it is possible to express the space Fourier transforms of spin-isospin–averaged baryon density, scalar density and vector density fluctuations for protons and neutrons in terms of the density matrix as

$$\begin{pmatrix} \delta\vec{\rho}_{\alpha,{\rm v}}(\vec{k},t) \\ \delta\rho_{\alpha,{\rm s}}(\vec{k},t) \\ \delta\rho_{\alpha,{\rm b}}(\vec{k},t) \end{pmatrix} = \gamma\sum_{\lambda\lambda'}\int\frac{{\rm d}^3p}{(2\pi\hbar)^3}\begin{pmatrix} \vec{\xi}^{\rm v}_{\lambda'\lambda}(\vec{p}_2,\vec{p}_1) \\ \xi^{\rm s}_{\lambda'\lambda}(\vec{p}_2,\vec{p}_1) \\ \xi^{\rm b}_{\lambda'\lambda}(\vec{p}_2,\vec{p}_1) \end{pmatrix} \times\delta\rho_{\alpha,\lambda'\lambda}(\vec{p}_2,\vec{p}_1,t), \quad (20)$$

where $\gamma = 2$ is the spin factor, $\vec{p}_2 = \vec{p} + \hbar\vec{k}/2$ and $\vec{p}_1 = \vec{p} - \hbar\vec{k}/2$.

We solve eqs. (18) and (19) by employing the standard method of the one-sided Fourier transform in time to obtain [16]

$$\delta\tilde{\rho}_{p,\lambda'\lambda}(\vec{p}_2,\vec{p}_1,\omega) - X_{p,\lambda'\lambda}(\vec{k},\omega)\left[\frac{n_{p,\lambda'}(\vec{p}_2)-n_{p,\lambda}(\vec{p}_1)}{\hbar\omega-[\lambda' e^*(p_2)-\lambda e^*(p_1)]}\right] = i\hbar\frac{\delta\rho_{p,\lambda'\lambda}(\vec{p}_2,\vec{p}_1,0)}{\hbar\omega-[\lambda' e^*(p_2)-\lambda e^*(p_1)]} \quad (21)$$

and

$$\delta\tilde{\rho}_{n,\lambda'\lambda}(\vec{p}_2,\vec{p}_1,\omega) - X_{n,\lambda'\lambda}(\vec{k},\omega)\left[\frac{n_{n,\lambda'}(\vec{p}_2)-n_{n,\lambda}(\vec{p}_1)}{\hbar\omega-[\lambda' e^*(p_2)-\lambda e^*(p_1)]}\right] = i\hbar\frac{\delta\rho_{n,\lambda'\lambda}(\vec{p}_2,\vec{p}_1,0)}{\hbar\omega-[\lambda' e^*(p_2)-\lambda e^*(p_1)]}. \quad (22)$$

In these expressions $\delta\rho_{\alpha,\lambda'\lambda}(\vec{p}_2,\vec{p}_1,0)$ denotes fluctuations of proton and neutron density matrices at the initial state, and the quantities $X_{p,\lambda'\lambda}(\vec{k},\omega)$ and $X_{n,\lambda'\lambda}(\vec{k},\omega)$ are given by

$$\begin{aligned} X_{p,\lambda'\lambda}(\vec{k},\omega) = {} & G_{\rm s}^2\xi^{\rm s}_{\lambda'\lambda}\delta\tilde{\rho}_{\rm s}(\vec{k},\omega) \\ & -G_{\rm v}^2\left[\xi^{\rm b}_{\lambda'\lambda}\delta\tilde{\rho}_{\rm b}(\vec{k},\omega)-\vec{\xi}^{\rm v}_{\lambda'\lambda}\cdot\delta\vec{\tilde{\rho}}_{\rm v}(\vec{k},\omega)\right] \\ & -G_{\rho}^2\left[\xi^{\rm b}_{\lambda'\lambda}\delta\tilde{\rho}_{3,0}(\vec{k},\omega)-\vec{\xi}^{\rm v}_{\lambda'\lambda}\cdot\delta\vec{\tilde{\rho}}_{3}(\vec{k},\omega)\right] \\ & -G_{\gamma}^2\left[\xi^{\rm b}_{\lambda'\lambda}\delta\tilde{\rho}_{p,b}(\vec{k},\omega)-\vec{\xi}^{\rm v}_{\lambda'\lambda}\cdot\delta\vec{\tilde{\rho}}_{p,{\rm v}}(\vec{k},\omega)\right] \end{aligned} \quad (23)$$

and

$$\begin{aligned} X_{n,\lambda'\lambda}(\vec{k},\omega) = {} & G_{\rm s}^2\xi^{\rm s}_{\lambda'\lambda}\delta\tilde{\rho}_{\rm s}(\vec{k},\omega) \\ & -G_{\rm v}^2\left[\xi^{\rm b}_{\lambda'\lambda}\delta\tilde{\rho}_{\rm b}(\vec{k},\omega)-\vec{\xi}^{\rm v}_{\lambda'\lambda}\cdot\delta\vec{\tilde{\rho}}_{\rm v}(\vec{k},\omega)\right] \\ & -G_{\rho}^2\left[\xi^{\rm b}_{\lambda'\lambda}\delta\tilde{\rho}_{3,0}(\vec{k},\omega)-\vec{\xi}^{\rm v}_{\lambda'\lambda}\cdot\delta\vec{\tilde{\rho}}_{3}(\vec{k},\omega)\right]. \end{aligned} \quad (24)$$

By carrying out one-sided Fourier transforms of linearized meson field equations, it is possible to eliminate fluctuating meson fields by expressing them in terms of fluctuating scalar, current and baryon density fluctuations. As a result, the effective coupling constants that appear in eqs. (23) and (24) are defined as

$$\begin{pmatrix} G_{\rm v}^2 \\ G_{\rm s}^2 \\ G_{\rho}^2 \\ G_{\gamma}^2 \end{pmatrix} = \begin{pmatrix} g_{\rm v}^2/[-(\omega/c)^2+k^2+\mu_{\rm v}^2] \\ g_{\rm s}^2/[-(\omega/c)^2+k^2+\mu_{\rm v}^2-2g_2\phi_0-3g_3\phi_0^2] \\ g_{\rho}^2/4[-(\omega/c)^2+k^2+\mu_{\rho}^2] \\ e^2/[-(\omega/c)^2+k^2] \end{pmatrix}. \quad (25)$$

Multiplying both sides of eqs. (21) and (22) by $\xi^{\rm b}_{\lambda'\lambda}(\vec{p}_2,\vec{p}_1)$, $\xi^{\rm s}_{\lambda'\lambda}(\vec{p}_2,\vec{p}_1)$ and $\vec{\xi}^{\rm v}_{\lambda'\lambda}(\vec{p}_2,\vec{p}_1)$ and integrating over the momentum $\vec{p}$, we obtain six coupled algebraic equations for the Fourier transforms of the fluctuating baryon density, the scalar density and the vector density of protons and neutrons, which can be expressed in a convenient matrix form as

$$\begin{pmatrix} A_1^p & A_2^p & A_3^p & A_1^n & A_2^n & A_3^n \\ B_1^p & B_2^p & B_3^p & B_1^n & B_2^n & B_3^n \\ C_1^p & C_2^p & C_3^p & C_1^n & C_2^n & C_3^n \\ D_1^p & D_2^p & D_3^p & D_1^n & D_2^n & D_3^n \\ E_1^p & E_2^p & E_3^p & E_1^n & E_2^n & E_3^n \\ F_1^p & F_2^p & F_3^p & F_1^n & F_2^n & F_3^n \end{pmatrix}\begin{pmatrix} \delta\tilde{\rho}_p^{\rm v}(\vec{k},\omega) \\ \delta\tilde{\rho}_p^{\rm s}(\vec{k},\omega) \\ \delta\tilde{\rho}_p^{\rm b}(\vec{k},\omega) \\ \delta\tilde{\rho}_n^{\rm v}(\vec{k},\omega) \\ \delta\tilde{\rho}_n^{\rm s}(\vec{k},\omega) \\ \delta\tilde{\rho}_n^{\rm b}(\vec{k},\omega) \end{pmatrix} = i\hbar\begin{pmatrix} \tilde{S}_p^{\rm b}(\vec{k},\omega) \\ \tilde{S}_p^{\rm s}(\vec{k},\omega) \\ \tilde{S}_p^{\rm v}(\vec{k},\omega) \\ \tilde{S}_n^{\rm b}(\vec{k},\omega) \\ \tilde{S}_n^{\rm s}(\vec{k},\omega) \\ \tilde{S}_n^{\rm v}(\vec{k},\omega) \end{pmatrix}. \quad (26)$$

In this expression the coefficient matrix is given by

see eq. (27) *above*

with $P = G_{\rm v}^2 + G_\rho^2 + G_\gamma^2$, $Q = G_{\rm s}^2$, $G = G_{\rm v}^2 - G_\rho^2$ and $R = G_{\rm v}^2 + G_\rho^2$. The quantities χ's and $\tilde{\chi}$'s are the relativistic quantal Lindhard functions associated with baryon, scalar, vector mesons and cross-terms. These expressions are given in [10] for symmetric matter. For clarity of presentation, we also reproduce them here for charge-asymmetric nuclear matter as

$$\begin{pmatrix}\chi_\alpha^{\rm v}(\vec{k},\omega)\\ \chi_\alpha^{\rm s}(\vec{k},\omega)\\ \chi_\alpha^{\rm b}(\vec{k},\omega)\end{pmatrix} = \gamma\sum_{\lambda\lambda'}\int\frac{{\rm d}^3p}{(2\pi\hbar)^3}\begin{pmatrix}\xi_{\lambda'\lambda}^{\rm b}\xi_{\lambda'\lambda}^{\rm v}\\ \xi_{\lambda'\lambda}^{\rm b}\xi_{\lambda'\lambda}^{\rm s}\\ \xi_{\lambda'\lambda}^{\rm b}\xi_{\lambda'\lambda}^{\rm b}\end{pmatrix} \times\frac{n_{\alpha,\lambda'}(\vec{p}+\hbar\vec{k}/2)-n_{\alpha,\lambda}(\vec{p}-\hbar\vec{k}/2)}{\hbar\omega-[\lambda' e^*(\vec{p}+\hbar\vec{k}/2)-\lambda e^*(\vec{p}-\hbar\vec{k}/2)]} \tag{28}$$

and

$$\begin{pmatrix}\tilde{\chi}_\alpha^{\rm v}(\vec{k},\omega)\\ \tilde{\chi}_\alpha^{\rm s}(\vec{k},\omega)\\ \tilde{\chi}_\alpha^{\rm b}(\vec{k},\omega)\end{pmatrix} = \gamma\sum_{\lambda\lambda'}\int\frac{{\rm d}^3p}{(2\pi\hbar)^3}\begin{pmatrix}\xi_{\lambda'\lambda}^{\rm s}\xi_{\lambda'\lambda}^{\rm v}\\ \xi_{\lambda'\lambda}^{\rm s}\xi_{\lambda'\lambda}^{\rm s}\\ \xi_{\lambda'\lambda}^{\rm v}\xi_{\lambda'\lambda}^{\rm v}\end{pmatrix} \times\frac{n_{\alpha,\lambda'}(\vec{p}+\hbar\vec{k}/2)-n_{\alpha,\lambda}(\vec{p}-\hbar\vec{k}/2)}{\hbar\omega-[\lambda' e^*(\vec{p}+\hbar\vec{k}/2)-\lambda e^*(\vec{p}-\vec{k}/2)]}. \tag{29}$$

Since in our analysis we consider the longitudinal unstable modes, in these expressions we retain only the component of the vector density fluctuations in the propagation direction and use the notation, $\delta\tilde{\rho}_\alpha^{\rm v}(\vec{k},\omega) = \delta\tilde{\vec{\rho}}_\alpha^{\rm v}(\vec{k},\omega)\cdot\vec{k}$ and $\tilde{\xi}_\alpha^{\rm v} = \tilde{\vec{\xi}}_\alpha^{\rm v}\cdot\vec{k}$. The source terms in eq. (26) are given by

$$\begin{pmatrix}\tilde{S}_\alpha^{\rm v}(\vec{k},\omega)\\ \tilde{S}_\alpha^{\rm s}(\vec{k},\omega)\\ \tilde{S}_\alpha^{\rm b}(\vec{k},\omega)\end{pmatrix} = \gamma\sum_{\lambda\lambda'}\int\frac{{\rm d}^3p}{(2\pi\hbar)^3}\begin{pmatrix}\xi_{\lambda'\lambda}^{\rm v}\\ \xi_{\lambda'\lambda}^{\rm s}\\ \xi_{\lambda'\lambda}^{\rm b}\end{pmatrix} \times\frac{\delta\rho_{\alpha,\lambda'\lambda}(\vec{p}+\hbar\vec{k}/2,\vec{p}-\hbar\vec{k}/2)}{\hbar\omega-[\lambda' e^*(\vec{p}+\hbar\vec{k}/2)-\lambda e^*(\vec{p}-\hbar\vec{k}/2)]}, \tag{30}$$

where $\delta\rho_{\alpha,\lambda'\lambda}(\vec{p}+\hbar\vec{k}/2,\vec{p}-\hbar\vec{k}/2) = \delta\rho_{\alpha,\lambda'\lambda}(\vec{p}+\hbar\vec{k}/2,\vec{p}-\hbar\vec{k}/2,0)$ denotes the initial fluctuations of the single-particle density matrix. We note that the semi-classical limits of eqs. (28)–(30) are obtained by retaining only the positive-energy sector $(\lambda,\lambda') = (+,+)$ and keeping the lowest-order terms in the integrands in the wave number $\vec{k}$ [8–10]. We can solve the algebraic equation (26) for the proton and neutron baryon density fluctuations to give

$$\delta\tilde{\rho}_\alpha^b(\vec{k},\omega) = \frac{i\hbar}{\varepsilon(\vec{k},\omega)}\Big[N_1^\alpha\tilde{S}_p^{\rm b} - N_2^\alpha\tilde{S}_p^{\rm s} + N_3^\alpha\tilde{S}_p^{\rm v} - N_4^\alpha\tilde{S}_n^{\rm b} - N_5^\alpha\tilde{S}_n^{\rm s} + N_6^\alpha\tilde{S}_n^{\rm v}\Big], \tag{31}$$

where the quantity $\varepsilon(\vec{k},\omega)$ denotes the susceptibility. The expressions for the susceptibility and the expansion coefficients N_j^α, for $j = 1,2,3,4$ are given in appendix A.

3 Early growth of density fluctuations

We can determine the time development of baryon density fluctuations by taking the inverse Fourier transform of eq. (31) in time. We can calculate the inverse Fourier transform with the help of residue method. According to the residue method, we need to consider the poles arising from the susceptibility and source terms $\tilde{S}_\alpha^{\rm b}, \tilde{S}_\alpha^{\rm s}$ and $\tilde{S}_\alpha^{\rm v}$ in eq. (31). Non-collective poles are important for specifying density fluctuations at the initial state, however density fluctuations arising from these poles do not grow in time. Therefore, we neglect non-collective poles of the susceptibility and poles of the source terms, and retain dominant contributions to the growth of instabilities due to the collective poles of the susceptibility. By including only the growing and decaying collective unstable modes, we find

$$\delta\tilde{\rho}_\alpha^b(\vec{k},t) = \delta\rho_\alpha^+(\vec{k})e^{+\Gamma_k t} + \delta\rho_\alpha^-(\vec{k})e^{-\Gamma_k t}, \tag{32}$$

where the quantities

$$\delta\rho_\alpha^\mp(\vec{k}) = -\hbar\times\left\{\frac{N_1^\alpha\tilde{S}_p^{\rm b} - N_2^\alpha\tilde{S}_p^{\rm s} + N_3^\alpha\tilde{S}_p^{\rm v} - N_4^\alpha\tilde{S}_n^{\rm b} - N_5^\alpha\tilde{S}_n^{\rm s} + N_6^\alpha\tilde{S}_n^{\rm v}]}{\partial\varepsilon(\vec{k},\omega)/\partial\omega}\right\}_{\omega=\mp i\Gamma_k} \tag{33}$$

denote Fourier transforms of density fluctuations associated with the growing and decaying collective modes at the initial state. Growth and decay rates of the collective modes are determined by the dispersion relation, $\epsilon(\vec{k},\omega) = 0 \rightarrow \mp i\Gamma_k$. Figure 1 shows quantal dispersion relations and the comparison with the semi-classical calculations for charge-asymmetric matter with asymmetry $I = (\rho_{n,0}^b - \rho_{p,0}^b)/(\rho_{n,0}^b + \rho_{p,0}^b) = 0.5$ at temperature $T = 1\,{\rm MeV}$ in the upper panel (a) and at temperature $T = 5\,{\rm MeV}$ in the lower panel (b) at two different densities $\rho = 0.2\rho_0$ and $\rho = 0.4\rho_0$. In the figure, solid lines are the results of quantal calculations while dashed lines are obtained in the semi-classical limit. In this figure and in the rest of the paper we employ the relativistic Walecka model with non-linear self-interactions of the scalar meson with NL3 parameters, which provides a consistent description for static and dynamical global nuclear properties [15]. We observe that the behavior of the dispersion relation of unstable modes at both temperatures is similar to those obtained in symmetric matter [10]. In semi-classical calculations for smaller densities, $\rho = 0.2\rho_0$, unstable modes extend over a broader range of wavelengths as compared to the results of quantal calculations for both temperatures. On the other hand, at higher densities, $\rho = 0.4\rho_0$, semi-classical and quantal calculations give nearly the same results at both temperatures. We notice that dispersion relations have a cut-off at long wavelengths which arise from the long-range electromagnetic interactions. Figure 2 shows quantal dispersion relations and the comparison with the semi-classical calculations for neutron-rich matter with charge asymmetry $I = 0.8$ under the similar conditions of fig. 1. As matter becomes more neutron rich, the range of unstable modes

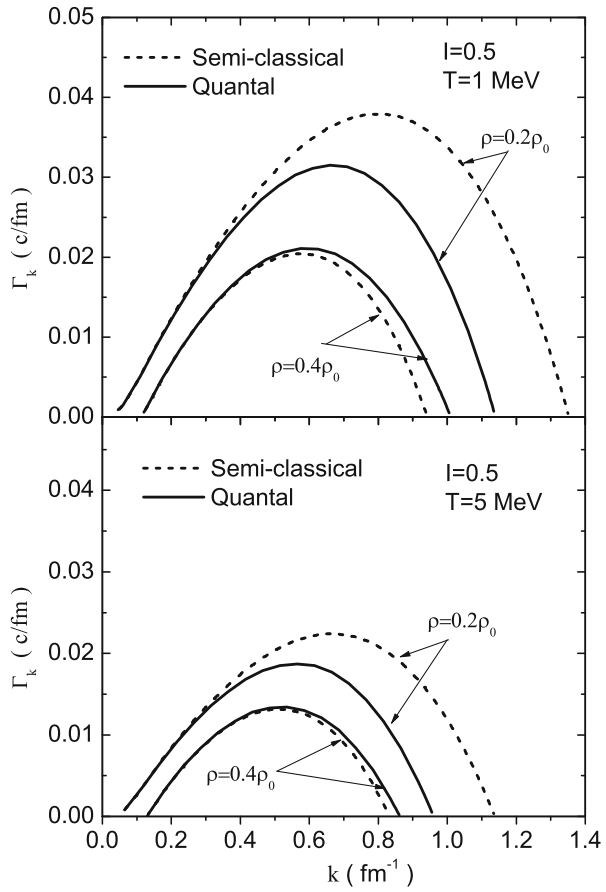

Fig. 1. Inverse growth rates of unstable modes as a function of the wave number for asymmetry $I = 0.5$ in quantal (solid lines) and semi-classical calculations (dashed lines) at $T = 1\,\mathrm{MeV}$ (upper panel) and at $T = 5\,\mathrm{MeV}$ (lower panel) for initial baryon densities $\rho = 0.2\rho_0$ and $\rho = 0.4\rho_0$.

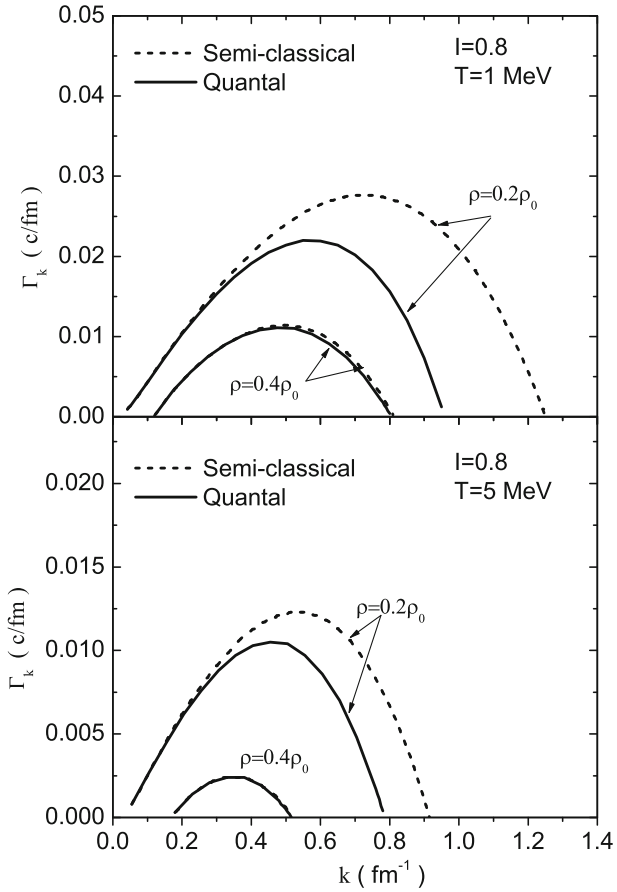

Fig. 2. The same as fig. 1 for charge asymmetry $I = 0.8$.

becomes narrower and growth rates of the most unstable modes are reduced. We note that the conditions in the upper panel of fig. 2, for $\rho = 0.4\rho_0$, approximately corresponds to the nuclear matter in the inner crust of neutron stars. Figure 3 illustrates the inverse growth rates of the most unstable collective modes in asymmetric matter with $I = 0.5$ and $I = 0.8$, respectively, as a function of the initial baryon density at two different temperatures $T = 1\,\mathrm{MeV}$ and $T = 5$ MeV. Solid lines and dashed lines are the results of quantal calculations and semi-classical calculations, respectively. At temperature $T = 5\,\mathrm{MeV}$, in both quantal and semi-classical calculations most unstable modes occur at densities in the vicinity of $\rho = 0.3\rho_0$. At the lower temperature of $T = 1\,\mathrm{MeV}$, quantal and semi-classical results exhibit similar behavior and most unstable modes shift toward lower densities around $\rho = 0.2\rho_0$. Also, we note that, at the densities and temperatures we consider, except small cut-off at the long wavelength edge, electro-magnetic interactions do not give any sizable contribution to the behavior of the dispersion relation and growth rates of unstable collective modes. Figure 4 shows phase boundaries of instabilities in neutron-rich matter of charge asymmetry $I = 0.8$ for a set of wavelengths in the temperature baryon density plane. Neutron-rich matter with $I = 0.8$ and $T = 1\,\mathrm{MeV}$, approximately corresponds to the structure of the crust of neutron stars. Under these conditions, limiting spinodal boundary occurs at baryon density $\rho = 0.5\rho_0$, which is consistent with the result found in [17].

The dispersion relation provides useful information about initial growth rates unstable modes, which are characterized by wave numbers or wavelengths. However, we can extract more useful information about dynamical evolution of the unstable system in the spinodal region from the equal time auto-correlation function of baryon density fluctuations. Here we consider only the baryon density correlation function. We define the equal time baryon density correlation functions between protons, neutrons and protons-neutrons in nuclear matter $\sigma_{\alpha\beta}(|\vec{r} - \vec{r}'|, t)$, $\alpha, \beta = p, n$, as follows:

$$\sigma_{\alpha\beta}(|\vec{r} - \vec{r}'|, t) = \overline{\delta\rho^b_\alpha(\vec{r}, t)\delta\rho^b_\beta(\vec{r}, t)} = \int \frac{\mathrm{d}^3k}{(2\pi)^3} e^{i\vec{k}\cdot\vec{x}} \tilde{\sigma}_{\alpha\beta}(\vec{k}, t). \quad (34)$$

Here $x = \vec{r} - \vec{r}'$ denotes the distance between two space locations and $\tilde{\sigma}_{\alpha\beta}(\vec{k}, t)$ is the spectral intensity of the baryon correlation functions. Spectral intensities are defined as the second moment of the Fourier transform of the baryon

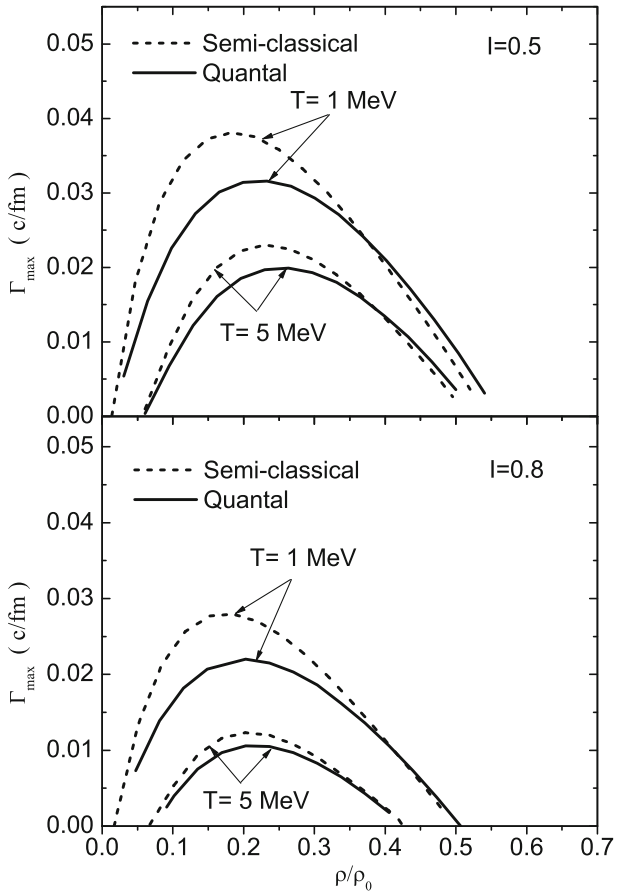

Fig. 3. Inverse growth rates of the most unstable collective modes in asymmetric matter with $I = 0.5$ (upper panel) and $I = 0.8$ (lower panel), respectively, as a function of the initial baryon density at two different temperatures $T = 1\,\mathrm{MeV}$ and $T = 5\,\mathrm{MeV}$. Solid lines and dashed lines are quantal and semi-classical calculations, respectively.

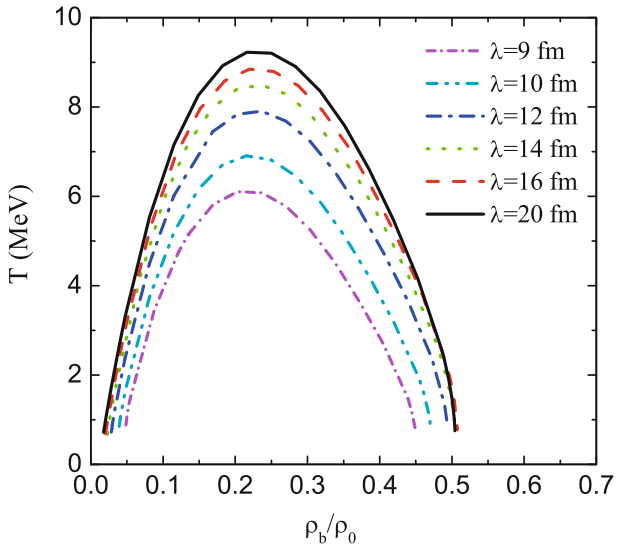

Fig. 4. Phase boundaries of instabilities in neutron-rich matter with $I = 0.8$ for a set of wavelengths in the temperature T and baryon density ρ_b plane.

density fluctuations according to

$$\overline{\delta\tilde{\rho}^b_\alpha(\vec{k},t)(\delta\tilde{\rho}^b_\beta(\vec{k}',t))^*} = (2\pi)^3\delta(\vec{k}-\vec{k}')\tilde{\sigma}_{\alpha\beta}(\vec{k},t), \quad (35)$$

where the bar denotes the ensemble averaged over the events generated in the SMF approach. Employing the expression (5) for the initial fluctuations in the plane wave representation, we can determine the spectral intensity of density correlation functions as follows [10]:

$$\tilde{\sigma}_{\alpha\beta}(\vec{k},t) = \hbar^2\frac{E^+_{\alpha\beta}(\vec{k})}{|[\partial\varepsilon(\vec{k},\omega)/\partial\omega]_{\omega=i\Gamma_k}|^2}(e^{+2\Gamma_k t}+e^{-2\Gamma_k t}) + \frac{2\hbar^2 E^-_{\alpha\beta}(\vec{k})}{|[\partial\varepsilon(\vec{k},\omega)/\partial\omega]_{\omega=i\Gamma_k}|^2}, \quad (36)$$

where the quantities symmetric $E^\pm_{\alpha\beta} = E^\mp_{\alpha\beta}$ for $\alpha = p, n$ are

$$\begin{aligned} E^\pm_{\alpha\alpha} = {} & K^{\pm p}_{\mathrm{bb}}|N^\alpha_1|^2 - 2K^{\pm p}_{\mathrm{bs}}(N^\alpha_1 N^\alpha_2) + K^{\pm p}_{\mathrm{ss}}|N^\alpha_2|^2 \\ & + K^{\pm p}_{\mathrm{vv}}|N^\alpha_3|^2 + K^{\pm n}_{\mathrm{bb}}|N^\alpha_4|^2 - 2K^{\pm n}_{\mathrm{bs}}(N^\alpha_4 N^\alpha_5) \\ & + K^{\pm n}_{\mathrm{ss}}|N^\alpha_5|^2 + K^{\pm n}_{\mathrm{vv}}|N^\alpha_6|^2 \end{aligned} \quad (37)$$

and, for $\alpha = p$, $\beta = n$,

$$\begin{aligned} E^\pm_{pn} = E^\pm_{np} = {} & K^{\pm p}_{\mathrm{bb}}(N^p_1 N^n_1) + K^{\pm p}_{\mathrm{bs}}(N^p_2 N^n_1 + N^p_1 N^n_2) \\ & - K^{\pm p}_{\mathrm{ss}}(N^p_2 N^n_2) - K^{\pm p}_{\mathrm{vv}}(N^p_3 N^n_3) - K^{\pm n}_{\mathrm{bb}}(N^p_4 N^n_4) \\ & + K^{\pm n}_{\mathrm{bs}}(N^p_4 N^n_5 N_5 p N^n_4) - K^{\pm n}_{\mathrm{ss}}(N^p_5 N^n_5) \\ & - K^{\pm n}_{\mathrm{vv}}(N^p_6 N^n_6). \end{aligned} \quad (38)$$

In expressions (37) and (38) all $N^\alpha_j = N^\alpha_j(+i\Gamma_k)$ factors for $j = 1, 2, 3, 4$ are evaluated at $\omega = +i\Gamma_k$ and quantities $K^{\pm\alpha}$ are defined as

$$\begin{aligned} \begin{pmatrix} K^{\pm\alpha}_{\mathrm{bb}} \\ K^{\pm\alpha}_{\mathrm{ss}} \\ K^{\pm\alpha}_{\mathrm{vv}} \\ K^{\pm\alpha}_{\mathrm{bs}} \end{pmatrix} = {} & \gamma^2\sum_{\lambda\lambda'}\int\frac{\mathrm{d}^3p}{(2\pi\hbar)^3}\begin{pmatrix} \xi^{\mathrm{b}}_{\lambda'\lambda}\xi^{\mathrm{b}}_{\lambda'\lambda} \\ \xi^{\mathrm{s}}_{\lambda'\lambda}\xi^{\mathrm{s}}_{\lambda'\lambda} \\ \xi^{\mathrm{v}}_{\lambda'\lambda}\xi^{\mathrm{v}}_{\lambda'\lambda} \\ \xi^{\mathrm{b}}_{\lambda'\lambda}\xi^{\mathrm{s}}_{\lambda'\lambda} \end{pmatrix} \\ & \times\frac{(\hbar\Gamma_k)^2 \pm [\lambda' e^*(\vec{p}_2) - \lambda e^*(\vec{p}_1)]^2}{\{(\hbar\Gamma_k)^2 + [\lambda' e^*(\vec{p}_2) - \lambda e^*(\vec{p}_1)]^2\}^2} \\ & \times n_{\alpha\lambda'}(\vec{p}_2)[1 - n_{\alpha\lambda}(\vec{p}_1)]. \end{aligned} \quad (39)$$

The initial value of the collective pole approximation for the density correlation function does not match the initial condition given in eq. (5). In fact, there are large deviations between the exact initial value and the initial value of the expression obtained by pole approximation, in particular for short wavelengths, since the approximate expression diverges as Γ_k goes to zero. As shown in [18], the exact expression of initial fluctuations can be reproduced by including non-collective poles in the evaluation of the inverse Fourier transform of expression (31) by the residue method. It is also shown, in the same reference, that fluctuations due to non-collective poles do not grow in time. Since the dominant contribution to baryon correlation functions for k integration in eq. (34) arises from the

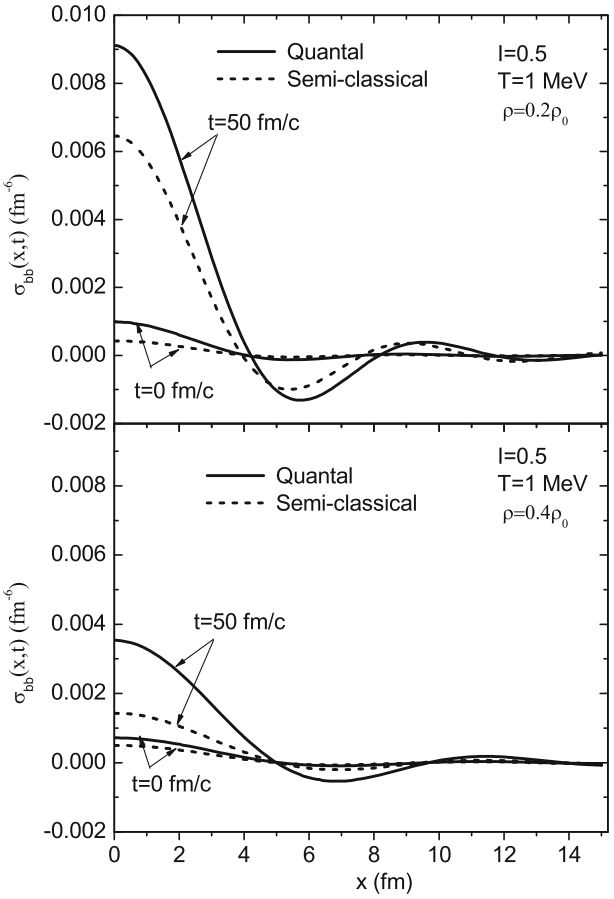

Fig. 5. Baryon density correlation functions for $I = 0.5$ at temperature $T = 1\,\mathrm{MeV}$ as function of the distance $x = \vec{r} - \vec{r}'$ between two space locations at initial densities $\rho = 0.2\rho_0$ (upper panel) and $\rho = 0.4\rho_0$ (lower panel). The correlation functions in quantal (solid lines) and semi-classical (dashed lines) calculations are indicated at initial time $t = 0$ and at time $t = 40\,\mathrm{fm}/c$, respectively.

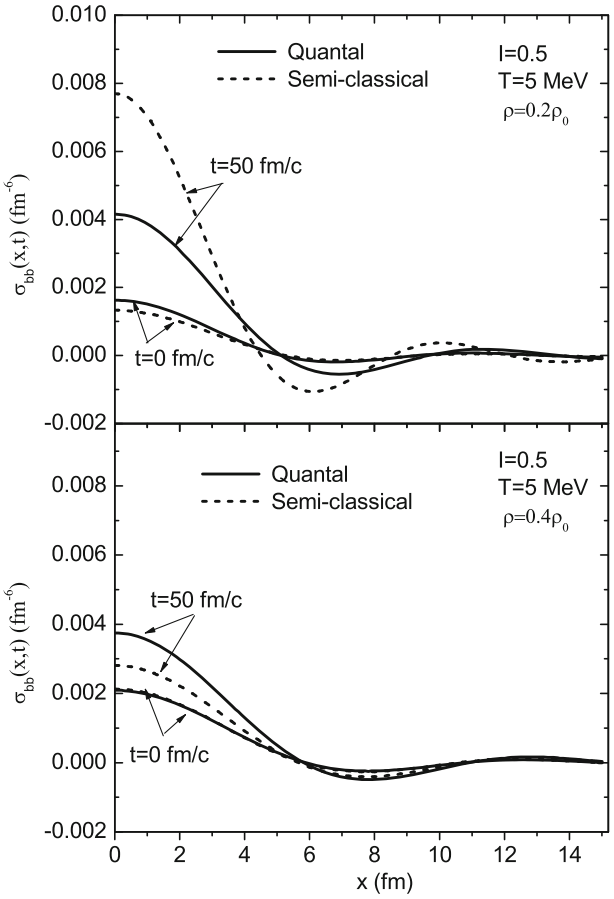

Fig. 6. The same as fig. 5 for temperature $T = 5\,\mathrm{MeV}$.

most unstable regions in figs. 1 and 2, we carry out the integration in eq. (34) up to a k_{cut}. This cut-off value is taken sufficiently below the singular behavior of $\tilde{\sigma}_{\alpha\beta}(\vec{k}, t = 0)$.

The total baryon density correlation function is given as the sum of proton, neutron correlation functions and the cross-correlations according to

$$\sigma(|\vec{r} - \vec{r}'|, t) = \sigma_{pp}(|\vec{r} - \vec{r}'|, t) + \sigma_{nn}(|\vec{r} - \vec{r}'|, t) + 2\sigma_{pn}(|\vec{r} - \vec{r}'|, t). \quad (40)$$

Figures 5 and 6 illustrate the baryon density correlation functions for $I = 0.5$ at two different temperatures, $T = 1\,\mathrm{MeV}$, $T = 5\,\mathrm{MeV}$, as a function of the distance $x = \vec{r} - \vec{r}'$ between two space locations at two different initial densities $\rho = 0.2\rho_0$ (upper panels) and $\rho = 0.4\rho_0$ (lower panels). The correlation functions are calculated at the initial time $t = 0$ and at time $t = 50\,\mathrm{fm}/c$, and the results of the quantal and semi-classical calculations are indicated by solid and dashed lines, respectively. Figure 7 shows a similar graph for neutron-rich matter with $I = 0.8$ at temperature $T = 1\,\mathrm{MeV}$, which approximately corresponds to the conditions in the crust of neutron stars. The evolution of the baryon density correlation function provides useful information about the size of initial condensation regions and the time scale of the condensation mechanism. We define the typical size of the initial condensation region as the width of the correlation function at half maximum, which is referred to as the correlation length x_{cor}. Qualitative behavior of baryon correlation function for asymmetric matter presented here is rather similar to the symmetric matter presented in [10]. However, we notice that the baryon density fluctuations grow slower for increasing charge asymmetry of the matter. For example, at $T = 1\,\mathrm{Mev}$ and $\rho = 0.4\rho_0$, fluctuations grow four times slower in neutron-rich matter $I = 0.8$ than in $I = 0.5$. Although it somewhat depends on the k_{cut} introduced in the integration in eq. (34), we observe at low temperature $T = 1\,\mathrm{MeV}$ in figs. 5 and 7, a large quantal effect in the initial growth of the density correlation function. We can understand this effect by noticing that at zero temperature, the semi-classical expression vanishes $n_{\alpha\lambda}(\vec{p})[1 - n_{\alpha\lambda}(\vec{p}')] = 0$. Therefore the initial density correlation functions vanish and they do not grow in time at all $\sigma_{bb}(|\vec{r} - \vec{r}'|, t) = 0$. On the other hand, in quantal framework even at zero temperature, as a result zero point fluctuations of collective modes, $n_{\alpha\lambda}(\vec{p} + \hbar\vec{k}/2)[1 - n_{\alpha\lambda}(\vec{p} - \hbar\vec{k}/2)] \neq 0$, the den-

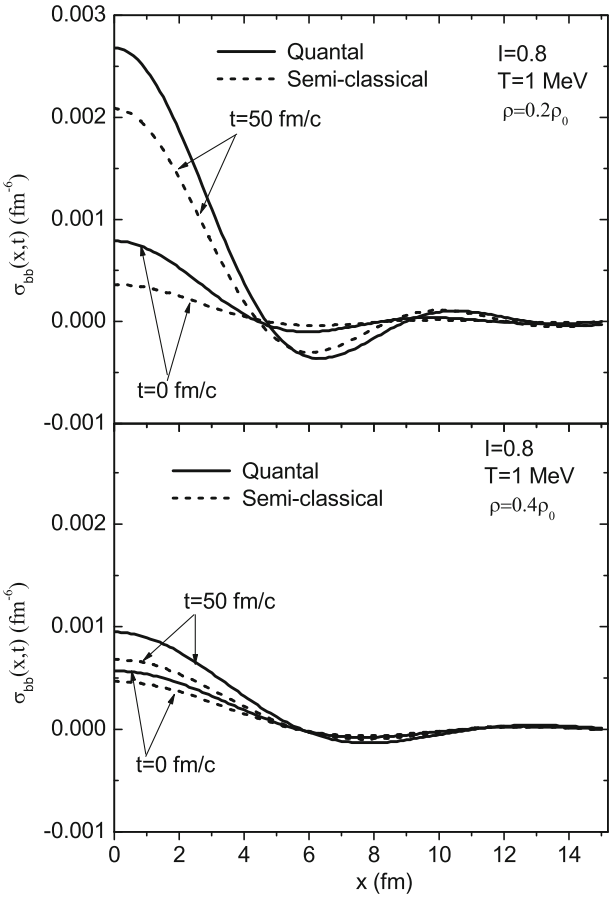

Fig. 7. The same as fig. 5 for charge asymmetry $I = 0.8$.

sity correlation function remains finite and grows in time. From these figures, the correlation lengths, which provide a measure for radius of the correlation volume, have a slight dependence on the temperature and the initial baryon density. In asymmetric matter with $I = 0.5$, the correlation length increases from about $x_{cor} = 2.5\,\mathrm{fm}$ at temperature $T = 1\,\mathrm{MeV}$ to about $x_{cor} = 3.0\,\mathrm{fm}$ at temperature $T = 5\,\mathrm{MeV}$ for both densities $\rho = 0.2\rho_0$ and $\rho = 0.4\rho_0$. In neutron-rich matter with $I = 0.8$ and temperature $T = 1\,\mathrm{MeV}$, it increases from about $x_{cor} = 2.0\,\mathrm{fm}$ at $\rho = 0.2\rho_0$ to $x_{cor} = 3.0\,\mathrm{fm}$ at $\rho = 0.4\rho_0$. The magnitudes of correlation radii extracted from the correlation functions are consistent with the quarter wavelengths of the most unstable modes in the dispersion relations with corresponding values of density and temperature.

4 Conclusion

In this work, we examine the early development of spinodal instabilities and baryon density correlation functions in charge-asymmetric nuclear matter employing the stochastic extension of the Walecka-type relativistic mean-field theory and including the coupling of baryon fields to the rho meson. We carry out these calculations in linear response frameworks of the relativistic mean-field theory in both quantal and semi-classical limits with NL3 parameterization of the model. We find that, at temperatures $T = 1\,\mathrm{MeV}$ and $T = 5\,\mathrm{MeV}$, and relatively low densities in the vicinity of $\rho = 0.2\rho_0$, for charge asymmetries $I = 0.5$ and 0.8 in quantal calculations, most unstable collective modes are shifted towards relatively longer wavelengths and concentrated over a narrower range, while, in semi-classical calculations, the modes extend over a broader range in the dispersion relation. On the other hand, we observe that at relatively higher densities, around $\rho = 0.4\rho_0$, quantal dispersion relations nearly coincide with those obtained in the semi-classical calculations at both temperatures and charge asymmetries. This result is different from the calculations we found in the non-relativistic approach using an effective Skyrme interaction [19], in which the quantal inverse growth rates of unstable modes remain below the semi-classical results even for relatively large baryon densities. We believe this is a relativistic effect, and it arises from the fact that in the dispersion relations the effects of the $(-,+)$ and $(+,-)$ sectors, which do not have a counterpart in the semi-classical calculations, become gradually more important in matter at larger densities and larger charge asymmetries. Consequently, quantal dispersion relations become very close to the those found in the semi-classical limit. Most unstable behavior of matter depends strongly on the temperature. In charge-asymmetric matter with $I = 0.5$ at temperature $T = 5\,\mathrm{MeV}$ (typical conditions during the expansion phase of heavy-ion collisions at energies around Fermi energy per nucleon) the fastest growth of instabilities occurs at densities around $\rho = 0.3\rho_0$. In neutron-rich matter with $I = 0.8$ at temperature $T = 1\,\mathrm{MeV}$ (typical conditions in the crust of neutron stars) the fastest growth of instabilities occurs at lower densities around $\rho = 0.2\rho_0$. The growth of baryon density correlation provides further information on the condensation mechanism during the early stages of liquid-gas transformation of the matter. There are two competing effects during the early growth of density fluctuations. At low temperatures around $T = 1\,\mathrm{MeV}$, the magnitude of initial density fluctuations is larger in the quantal calculations than in the semi-classical calculations, while at relatively higher temperatures, around $T = 5\,\mathrm{MeV}$, the initial fluctuations have nearly the same magnitude. On the other hand, the semi-classical inverse growth rates at low densities, around $\rho = 0.2\rho_0$, are larger than the quantal rates, while the growth rates are nearly the same at higher densities, around $\rho = 0.4\rho_0$, at both temperatures. As a result of these competing effects, baryon density fluctuations grow relatively faster in the quantal description than in the semi-classical approach at conditions considered in the calculations, except at low densities, around $\rho = 0.2\rho_0$, and higher temperatures, around $T = 5\,\mathrm{MeV}$, where the quantal growth occurs at a slower rate. We also note that typical sizes of early condensation regions extracted from baryon density correlation functions are consistent with those found from dispersion relations of the unstable collective modes. In this work we carry out investigations of

growth of the spin-averaged baryon density fluctuations in nuclear matter. We should note that spin instabilities may play a crucial role in the condensation mechanism especially in the inner crust of neutron stars.

SA gratefully acknowledges TUBITAK for a partial support and METU for the warm hospitality extended to him during his visit. This work is supported in part by the US DOE grant No. DE-FG05-89ER40530 and in part by TUBITAK grant No. 110T274.

Appendix A.

The susceptibility $\varepsilon(\vec{k},\omega)$ can be expressed as 6×6 determinant with elements determined by eqs. (20) and (21) as

$$\varepsilon(\vec{k},\omega)=\begin{vmatrix} A_1^p & A_2^p & A_3^p & A_1^n & A_2^n & A_3^n \\ B_1^p & B_2^p & B_3^p & B_1^n & B_2^n & B_3^n \\ C_1^p & C_2^p & C_3^p & C_1^n & C_2^n & C_3^n \\ D_1^p & D_2^p & D_3^p & D_1^n & D_2^n & D_3^n \\ E_1^p & E_2^p & E_3^p & E_1^n & E_2^n & E_3^n \\ F_1^p & F_2^p & F_3^p & F_1^n & F_2^n & F_3^n \end{vmatrix}. \tag{A.1}$$

The expansion coefficients N_j^α for $j=1,2,3,4$, in eq. (23), can be given as 5×5 determinants as

$$N_1^p=\begin{vmatrix} B_1^p & B_2^p & B_1^n & B_2^n & B_3^n \\ C_1^p & C_2^p & C_1^n & C_2^n & C_3^n \\ D_1^p & D_2^p & D_1^n & D_2^n & D_3^n \\ E_1^p & E_2^p & E_1^n & E_2^n & E_3^n \\ F_1^p & F_2^p & F_1^n & F_2^n & F_3^n \end{vmatrix},\quad N_2^p=\begin{vmatrix} A_1^p & A_2^p & A_1^n & A_2^n & A_3^n \\ C_1^p & C_2^p & C_1^n & C_2^n & C_3^n \\ D_1^p & D_2^p & D_1^n & D_2^n & D_3^n \\ E_1^p & E_2^p & E_1^n & E_2^n & E_3^n \\ F_1^p & F_2^p & F_1^n & F_2^n & F_3^n \end{vmatrix},$$

$$N_3^p=\begin{vmatrix} A_1^p & A_2^p & A_1^n & A_2^n & A_3^n \\ B_1^p & B_2^p & B_1^n & B_2^n & B_3^n \\ D_1^p & D_2^p & D_1^n & D_2^n & D_3^n \\ E_1^p & E_2^p & E_1^n & E_2^n & E_3^n \\ F_1^p & F_2^p & F_1^n & F_2^n & F_3^n \end{vmatrix}, \tag{A.2}$$

$$N_4^p=\begin{vmatrix} A_1^p & A_2^p & A_1^n & A_2^n & A_3^n \\ B_1^p & B_2^p & B_1^n & B_2^n & B_3^n \\ C_1^p & C_2^p & C_1^n & C_2^n & C_3^n \\ E_1^p & E_2^p & E_1^n & E_2^n & E_3^n \\ F_1^p & F_2^p & F_1^n & F_2^n & F_3^n \end{vmatrix},\quad N_5^p=\begin{vmatrix} A_1^p & A_2^p & A_1^n & A_2^n & A_3^n \\ B_1^p & B_2^p & B_1^n & B_2^n & B_3^n \\ C_1^p & C_2^p & C_1^n & C_2^n & C_3^n \\ D_1^p & D_2^p & D_1^n & D_2^n & D_3^n \\ F_1^p & F_2^p & F_1^n & F_2^n & F_3^n \end{vmatrix},$$

$$N_6^p=\begin{vmatrix} A_1^p & A_2^p & A_1^n & A_2^n & A_3^n \\ B_1^p & B_2^p & B_1^n & B_2^n & B_3^n \\ C_1^p & C_2^p & C_1^n & C_2^n & C_3^n \\ D_1^p & D_2^p & D_1^n & D_2^n & D_3^n \\ E_1^p & E_2^p & E_1^n & E_2^n & E_3^n \end{vmatrix}, \tag{A.3}$$

$$N_1^n=\begin{vmatrix} B_1^p & B_2^p & B_3^p & B_1^n & B_2^n \\ C_1^p & C_2^p & C_3^p & C_1^n & C_2^n \\ D_1^p & D_2^p & D_3^p & D_1^n & D_2^n \\ E_1^p & E_2^p & E_3^p & E_1^n & E_2^n \\ F_1^p & F_2^p & F_3^p & F_1^n & F_2^n \end{vmatrix},\quad N_2^n=\begin{vmatrix} A_1^p & A_2^p & A_3^p & A_1^n & A_2^n \\ C_1^p & C_2^p & C_3^p & C_1^n & C_2^n \\ D_1^p & D_2^p & D_3^p & D_1^n & D_2^n \\ E_1^p & E_2^p & E_3^p & E_1^n & E_2^n \\ F_1^p & F_2^p & F_3^p & F_1^n & F_2^n \end{vmatrix},$$

$$N_3^n=\begin{vmatrix} A_1^p & A_2^p & A_3^p & A_1^n & A_2^n \\ B_1^p & B_2^p & B_3^p & B_1^n & B_2^n \\ D_1^p & D_2^p & D_3^p & D_1^n & D_2^n \\ E_1^p & E_2^p & E_3^p & E_1^n & E_2^n \\ F_1^p & F_2^p & F_3^p & F_1^n & F_2^n \end{vmatrix}, \tag{A.4}$$

$$N_4^n=\begin{vmatrix} A_1^p & A_2^p & A_3^p & A_1^n & A_2^n \\ B_1^p & B_2^p & B_3^p & B_1^n & B_2^n \\ C_1^p & C_2^p & C_3^p & C_1^n & C_2^n \\ E_1^p & E_2^p & E_3^p & E_1^n & E_2^n \\ F_1^p & F_2^p & F_3^p & F_1^n & F_2^n \end{vmatrix},\quad N_5^n=\begin{vmatrix} A_1^p & A_2^p & A_3^p & A_1^n & A_2^n \\ B_1^p & B_2^p & B_3^p & B_1^n & B_2^n \\ C_1^p & C_2^p & C_3^p & C_1^n & C_2^n \\ D_1^p & D_2^p & D_3^p & D_1^n & D_2^n \\ F_1^p & F_2^p & F_3^p & F_1^n & F_2^n \end{vmatrix},$$

$$N_6^n=\begin{vmatrix} A_1^p & A_2^p & A_3^p & A_1^n & A_2^n \\ B_1^p & B_2^p & B_3^p & B_1^n & B_2^n \\ C_1^p & C_2^p & C_3^p & C_1^n & C_2^n \\ D_1^p & D_2^p & D_3^p & D_1^n & D_2^n \\ E_1^p & E_2^p & E_3^p & E_1^n & E_2^n \end{vmatrix}. \tag{A.5}$$

Elements of these determinants N_j^α are also determeined by eqs. (20) and (21).

References

1. S. Ayik, Phys. Lett. B **658**, 174 (2008).
2. R. Balian, M. Veneroni, Phys. Lett. B **136**, 301 (1984).
3. S. Ayik, K. Washiyama, D. Lacroix, Phys. Rev. C **79**, 054606 (2009).
4. K. Washiyama, S. Ayik, D. Lacroix, Phys. Rev. C **80**, 031602 (2009).
5. S. Ayik, B. Yilmaz, D. Lacroix, Phys. Rev. C **81**, 034605 (2010).
6. D. Lacroix, S. Ayik, B. Yilmaz, Phys. Rev. C **85**, 041602 (2012).
7. Ph. Chomaz, M. Colonna, J. Randrup, Phys. Rep. **389**, 263 (2004).
8. S. Ayik, O. Yilmaz, N. Er, A. Gokalp, P. Ring, Phys. Rev. C **80**, 034613 (2009).
9. S. Ayik, O. Yilmaz, F. Acar, B Danisman, N. Er, A. Gokalp, Phys. Rev. C **80**, 034613 (2011).
10. O. Yilmaz, S. Ayik, A. Gokalp, Eur. Phys. J. A **47**, 123 (2011).
11. P. Ring, Prog. Part. Nucl. Phys. **37**, 193 (1996).
12. B.D. Serot, J.D. Walecka, Int. J. Mod. Phys. E **6**, 515 (1997).

13. P. Ring, Zhong-yu Ma, Nyguyen Van Giai, D. Vretenar, A. Wandelt, Li-gang Cao, Nucl. Phys. A **694**, 249 (2001).
14. D. Vretenar, A.V. Afanasjev, G.A. Lalazissis, P. Ring, Phys. Rep. **409**, 101 (2005).
15. G.A. Lalazissis, J. Konig, P. Ring, Phys. Rev. C **55**, 540 (1997).
16. E.M. Lifshitz, L.P. Pitaevskii, *Physical Kinetics* (Pergamon, 1981).
17. J. Xu, C.M. Ko, Phys. Rev. C **82**, 044311 (2010).
18. P. Bozek, Phys. Rev. Lett. B **383**, 121 (1996).
19. S. Ayik, N. Er, O. Yilmaz, A. Gokalp, Nucl. Phys. A **812**, 44 (2008).